

# Enhancement of $Y_D^\bullet$ spin relaxation by the $CaMn_4$ cluster in photosystem II detected at room temperature: A new probe for the S-cycle

Felix M. Ho<sup>a,\*</sup>, Susan F. Morvaridi<sup>b</sup>, Fikret Mamedov<sup>a</sup>, Stenbjörn Styring<sup>a,\*</sup>

<sup>a</sup> Molecular Biomimetics, Department of Photochemistry and Molecular Science, Ångström Laboratory, P.O. Box 523, Uppsala University, SE-751 20 Uppsala, Sweden

<sup>b</sup> Department of Biochemistry, Centre for Chemistry and Chemical Engineering, Lund University, P.O. Box 124, SE-221 00 Lund, Sweden

Received 25 April 2006; received in revised form 17 July 2006; accepted 17 August 2006

Available online 22 August 2006

## Abstract

The long-lived, light-induced radical  $Y_D^\bullet$  of the Tyr161 residue in the D2 protein of Photosystem II (PSII) is known to magnetically interact with the  $CaMn_4$  cluster, situated  $\sim 30$  Å away. In this study we report a transient step-change increase in  $Y_D^\bullet$  EPR intensity upon the application of a single laser flash to  $S_1$  state-synchronised PSII-enriched membranes from spinach. This transient effect was observed at room temperature and high applied microwave power (100 mW) in samples containing PpBQ, as well as those containing DCMU. The subsequent decay lifetimes were found to differ depending on the additive used. We propose that this flash-induced signal increase was caused by enhanced spin relaxation of  $Y_D^\bullet$  by the OEC in the  $S_2$  state, as a consequence of the single laser flash turnover. The post-flash decay reflected  $S_2 \rightarrow S_1$  back-turnover, as confirmed by their correlations with independent measurements of  $S_2$  multiline EPR signal and flash-induced variable fluorescence decay kinetics under corresponding experimental conditions. This flash-induced effect opens up the possibility to study the kinetic behaviour of S-state transitions at room temperature using  $Y_D^\bullet$  as a probe.

© 2006 Elsevier B.V. All rights reserved.

**Keywords:** Photosystem II; EPR; Oxygen evolving complex; S-state transitions; Tyrosine D; Spin relaxation

## 1. Introduction

Photosystem II (PSII) catalyses the oxidation of water into molecular oxygen in photosynthetic plants, algae and cyanobacteria. At the heart of the process is the oxygen evolving centre (OEC) which consists of a  $CaMn_4$  cluster and a nearby Tyr 161 tyrosine residue on the D1 protein, known as  $Y_Z$  (see [1,2] for specialised journal issues on the subject; [3–9]). Upon illumination, the PSII reaction centre P680 is oxidised, and the electron is passed to Photosystem I via pheophytin and quinone

co-factors. The oxidised P680 is re-reduced by  $Y_Z$ , and the resulting radical is in turn reduced by the  $CaMn_4$  cluster. In this manner, the  $CaMn_4$  cluster acts as a cyclic “charge accumulator”, undergoing one-step oxidations at each photoreaction [1–4,9]. The cluster cycles through five intermediate oxidation states, collectively known as the S-states, and individually named  $S_0$  to  $S_4$ .  $S_0$  is the most reduced state, while  $S_1$  is the most dark-stable state. The  $S_2$  and  $S_3$  states are metastable states that decay back to  $S_1$  if they are not further oxidised to higher S-states.  $S_4$  is a transient state, which has not yet been directly observed, but it is during the spontaneous  $S_4 \rightarrow S_0$  transition that molecular oxygen is released from the oxidation of water. Although possible intermediates corresponding to the  $S_4$  state have recently been observed [10,11], their identities, and indeed the underlying conception of the S-cycle itself, are currently under debate [12].

While  $Y_Z$  is directly involved in the electron transfer reactions during water oxidation,  $Y_D$ , the symmetrically located Tyr 161 on the D2 protein (Tyr 160 in cyanobacteria), is not. However,  $Y_D$  forms a long-lived radical ( $Y_D^\bullet$ ) upon exposure to

**Abbreviations:** PSII, Photosystem II; OEC, oxygen evolving centre; P680, the primary donor in PSII;  $Q_A$  and  $Q_B$ , primary and secondary quinone acceptors in PSII;  $Y_Z$  and  $Y_Z^\bullet$ , tyrosine 161 of the PSII D1 polypeptide and its radical;  $Y_D$  and  $Y_D^\bullet$ , tyrosine 161 of the PSII D2 polypeptide and its radical; EPR, electron paramagnetic resonance; PpBQ, phenyl-*p*-benzoquinone; DCMU, 3-(3',4'-dichlorophenyl)-1,1-dimethylurea; DMSO, dimethylsulfoxide;  $t_{1/2}$ , half-life of decay

\* Corresponding authors. Tel.: +46 18 4716580; fax: +46 18 4719885.

E-mail addresses: [Felix.Ho@fotomol.uu.se](mailto:Felix.Ho@fotomol.uu.se) (F.M. Ho), [Stenbjorn.Styring@fotomol.uu.se](mailto:Stenbjorn.Styring@fotomol.uu.se) (S. Styring).

light [13–15], and this radical can be readily detected using EPR spectroscopy. The spin relaxation behaviour of  $Y_D^\bullet$  has been studied at low temperatures and shown to be affected by the  $CaMn_4$  cluster in an S-state dependent manner [16–24]. However, these experiments involved S-state intermediates that had been “frozen-in” *ex situ* prior to measurement. Therefore, kinetic information of the S-state transition process itself could not be gathered, and post-transition behaviours could not be observed. In addition, since the  $Y_D^\bullet$  spin-lattice relaxation rate is temperature-dependent [17–19,21–23], the results at cryogenic temperatures may also differ from those under physiological conditions.

The question to be investigated in this study was therefore whether or not it would be possible to exploit the differences in  $Y_D^\bullet$  spin relaxation rates under the influence of different S-states of the OEC to retrieve such information at room temperature. In particular, EPR was chosen to monitor the changes in  $Y_D^\bullet$  signal under conditions of high, saturating applied microwave power. Under non-saturating microwave power conditions, all radicals exhibit the same (double-integrated) signal intensity, independent of its spin relaxation rate. The number of radicals excited by the microwave would not be sufficient for differences in relaxation rates to influence the ground state population (and therefore the transition moment) significantly. By contrast, under saturating conditions, the populations of the upper and lower spin levels induced by Zeeman splitting are equal, and therefore no further absorption is possible even with increased applied microwave power. Therefore, the rate of spin relaxation from the upper spin level determines the maximum absorption achievable. A faster relaxing radical will give a more intense signal than a slower relaxing one. The S-state dependence of  $Y_D^\bullet$  spin relaxation rate thus presents the possibility of using  $Y_D^\bullet$  as a passive spectroscopic probe for kinetic measurements of S-state turnovers, thereby providing a new probe for the  $CaMn_4$  cluster during the S-cycle. We present here the first of such observations of  $Y_D^\bullet$  spin relaxation enhancement effects involving the flash-induced advancement from the  $S_1$  to the  $S_2$  state at room temperature.

## 2. Materials and methods

### 2.1. Sample preparation

PSII-enriched membranes were prepared under dim green light at 5 °C as described by Berthold et al. [25], with modifications as in Pace et al. [26]. The stock membrane samples were suspended in a buffer containing 25 mM MES, 400 mM sucrose, 3 mM  $MgCl_2$ , 15 mM NaCl at pH 6.1, and stored at –80 °C until required. EPR samples were prepared by diluting the stock suspension to 2 mg Chl/mL directly before use.

For Mn-depletion of PSII-enriched membranes, the sample was centrifuged, and the membrane pellet resuspended in 0.8 M Tris buffer, pH 8.0 [27]. This was stirred at room temperature for 20 min under room light, then centrifuged. The supernatant was removed, and the pellet was washed with the original buffer before being centrifuged again and resuspended in buffer.

### 2.2. EPR spectroscopy

Unless otherwise indicated, all procedures were performed at room temperature (~23 °C). Complete  $Y_D^\bullet$  oxidation was achieved by exposing the PSII-enriched membrane sample (2 mg Chl/mL) to room light for ~5 min.

Synchronisation of all PSII centres to the  $S_1$  state was obtained directly in the EPR flat sample cell using a preflash protocol as follows (adapted from Styring and Rutherford [28] and Åhring et al. [29]): the  $Y_D^\bullet$  oxidised sample was dark adapted on ice for 10 min, followed by the addition at room temperature of either PpBQ (50 mM in DMSO) to a final concentration of 0.5 mM, or of DCMU (5 mM in DMSO) to a final concentration of 0.15 mM, as required. The sample was then further dark adapted for 10 min at room temperature, during which time it was aspirated into a flat sample cell for EPR. The sample was given two saturating laser flashes, with the flashes separated by 12 min in the dark (Nd:YAG, 532 nm, 6 ns, 360 mJ/pulse), directly into the EPR spectrometer cavity at room temperature. A beam-spreader lens was placed in front of the cavity window to ensure that the entire window was illuminated by the laser light. The sample was then allowed to dark adapt for a further 12 min to achieve full synchronisation.

EPR measurements were performed using a Bruker Elexsys E580 spectrometer. Kinetic measurements of the  $Y_D^\bullet$  signal were performed by monitoring the EPR signal intensity at the downfield peak of  $Y_D^\bullet$  (inset in Fig. 1B). Single laser flashes were applied directly into the spectrometer cavity, and were electronically synchronised with EPR data collection using computer-controlled external triggering. For experiments involving PpBQ, individual laser flashes were separated by 12 min of darkness, whereas 21 s intervals were used for experiments involving DCMU.

For the quantification of the  $Y_D^\bullet$  intensity increase at the laser flash in the kinetic measurements, the signal increase was compared to a field scan  $Y_D^\bullet$  signal. To allow direct comparison, multiplicative scaling factors were applied to account for the different number of scans taken, conversion times, modulation amplitudes, signal gains and applied microwave powers in the respective experiments.

### 2.3. $S_2$ multiline signal measurements and variable fluorescence spectroscopy

For measurements of the  $S_2$  multiline EPR signal decay as a function of time at room temperature, PSII samples (2 mg Chl/mL) containing PpBQ (0.5 mM) were preflashed twice in standard EPR tubes (Nd:YAG, 532 nm, 10 ns, 200 mJ/pulse) and dark adapted for 12 min at room temperature as described above. As the laser flash was applied directly to the EPR tubes, no intervening beam-spreader lens was required. The flashes were saturating with respect to turnover to the  $S_2$  state (not shown). A single flash was then given to each sample to induce the  $S_2$  state. After the flash, the samples were incubated in the dark in a water bath (23 °C) for various times prior to freezing within 1 s in an ethanol/solid  $CO_2$  bath. They were then transferred to liquid nitrogen until the  $S_2$  multiline signal was measured at 7 K. Each sample was then immersed in a 200 K ethanol/solid  $CO_2$  bath and illuminated using light from a 800 W lamp filtered through a 4 cm  $CuSO_4$  solution. The  $S_2$  multiline signals were re-measured at 7 K.

Flash-induced variable fluorescence was measured with a PAM fluorimeter (Walz, Effeltrich, Germany) according to Mamedov et al. [30]. Samples containing 10 µg Chl/mL were dark adapted for 5 min, and DCMU was added to a final concentration of 10 µM. Single first flash measurements from 13 independent samples were averaged to give the fluorescence decay trace used for kinetics analysis.

## 3. Results

### 3.1. Observation of a microwave power-dependent, transient $Y_D^\bullet$ intensity increase

To monitor the intensity of the  $Y_D^\bullet$  EPR signal before and after the application of a laser flash, the signal intensity at the low field peak of  $Y_D^\bullet$  (bar in inset in Fig. 1B) was recorded as a function of time. It was found that upon the application of a laser flash to preflashed,  $S_1$  state-synchronised PSII membranes, a transient increase in the intensity of the  $Y_D^\bullet$  EPR signal could be observed at the higher applied microwave powers (Fig.

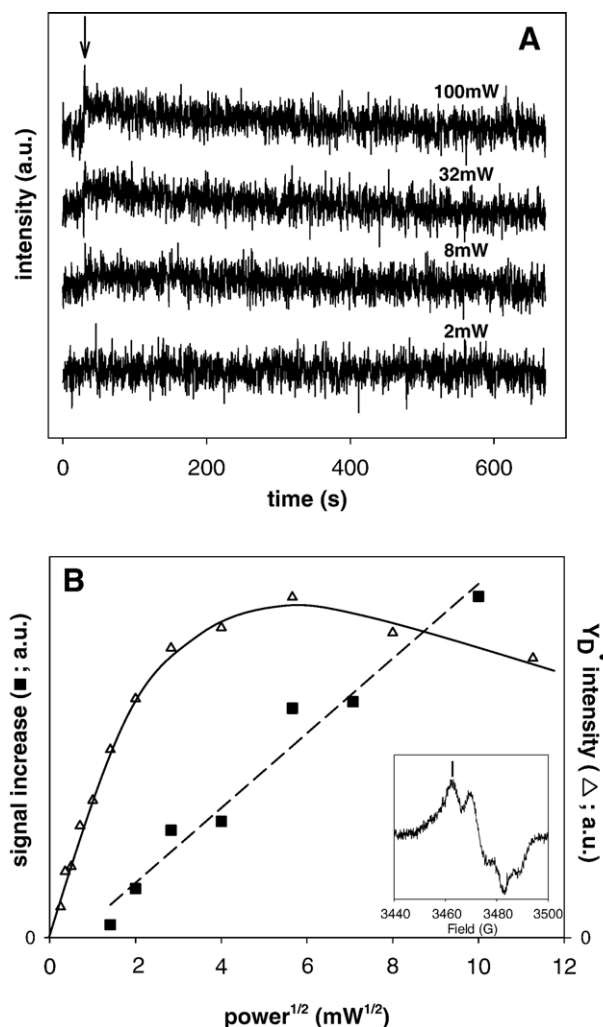


Fig. 1. (A) Flash-induced increase of the  $Y_D^{\bullet}$  EPR signal intensity at room temperature at different applied microwave powers. The  $S_1$  state-synchronised PSII-enriched membranes containing PpBQ were given a single laser flash (arrow) and then allowed to dark adapt. The applied microwave powers are shown above each trace. The inset in B shows a field scan of  $Y_D^{\bullet}$  and the bar marks the field at which the  $Y_D^{\bullet}$  intensity was monitored. (B) Comparison of the microwave power dependence of the magnitude of the transient flash-induced effect (filled squares, left axis; c.f. A) with the microwave power dependence of the  $Y_D^{\bullet}$  signal in dark adapted PSII-enriched membranes (open triangles, right axis). EPR spectrometer conditions: microwave frequency 9.77 GHz, modulation amplitude 6 G, modulation frequency 100 kHz. In addition, for A: conversion time 328 ms, time constant 82 ms, field position 3462 G (bar in inset), 4 flash transients summed for each trace. For B: each data point for the flash-induced effect was measured from a trace of 4 summed flash transients, as in A. The  $Y_D^{\bullet}$  power saturation curve was obtained by measurements of  $Y_D^{\bullet}$  spectra at microwave powers as given in the graph. For inset in B: microwave power 10 mW.

1A). There was a step-change in intensity coinciding with the laser flash, followed by a slow decay back to baseline levels. At low, non-saturating microwave powers (e.g. <2 mW), no such flash-induced signal increase could be observed, but it gradually appeared as the microwave power increased. In Fig. 1B, the amplitude of the flash-induced intensity increase (filled squares) is plotted as a function of the microwave power. It can be seen that the flash-induced change in signal amplitude increased concomitantly with increased microwave power. The trend was

approximately linear with respect to the square-root of the applied microwave power, over a wide range of microwave powers. The microwave power saturation curve of  $Y_D^{\bullet}$  in the dark is also shown in Fig. 1B for comparison (open triangles). It is interesting to note that although the  $Y_D^{\bullet}$  signal itself became saturated and decreased in intensity at microwave powers above ~30 mW, the flash-induced effect continued to increase in magnitude up to at least 100 mW.

### 3.2. Preflash protocol

The efficacy of the preflash protocol to synchronise all OEC's to the  $S_1$  state as well as to maintain full oxidation of  $Y_D$  as the  $Y_D^{\bullet}$  radical was verified by following the intensity of  $Y_D^{\bullet}$  as a function of time in the first three laser flashes after dark adaptation (Fig. 2A). This allowed the preflashing protocol in the presence of PpBQ to be monitored. To maximise the flash-induced increase, a microwave power of 100 mW was applied. The intensity of  $Y_D^{\bullet}$  was again measured at the low field peak (inset in Fig. 1B). The sample had first been in darkness for a total of 20 min after room light  $Y_D^{\bullet}$  oxidation, and the laser flashes (arrows) were applied at 12 min intervals.

After the first flash, the changes in the EPR signal of  $Y_D^{\bullet}$  occurred in three stages: (1) an immediate jump in signal intensity at the laser flash, as also seen in the microwave power experiments above (Fig. 1A), (2) a slower growth, and finally (3) an even slower decay. The second flash also gave a step-change increase at the laser flash, followed by a decay behaviour which was dominated by a slow decay, corresponding to the stage (3) of the first flash. However, a small contribution from a stage (2)-type slow increase could also be discerned. Following the third laser flash, only the slow decay stage (3) was observed after an initial intensity jump. The slow stage (2)-type signal increase was completely lacking. This behaviour was observed in all subsequent flashes.

The first flash and, to a smaller extent, the second flash trace also differed from subsequent traces in that the EPR signal did not return to the baseline level during the dark decay. Fig. 2B shows the results of the subtraction of the kinetic trace recorded after the third flash from the kinetic trace recorded after the first flash. This procedure thus removed the contributions from the reproducible, slow decay (stage (3)-type) present in all traces, as well as the step-change increase (stage (1)-type) at the laser flash, to the extent that it was present after the third flash. The difference revealed a gradual increase in  $Y_D^{\bullet}$  intensity, which thereafter remained stable. These results are indicative of oxidation of  $Y_D$  by higher S-states in a fraction of PSII centres during the first two flashes after dark-adaptation, as previously described [31,32] (see discussions below for a more detailed analysis). This persistent increase was also observed when the third flash trace was subtracted from the second flash trace, though the magnitude of the resulting difference was much smaller (not shown).

The flashed-induced behaviour became reproducible, not involving any  $Y_D$  oxidation, from the third flash onwards. Therefore, we concluded that two flashes were required to ensure full  $S_1$  synchronisation as well as full oxidation to  $Y_D^{\bullet}$ .

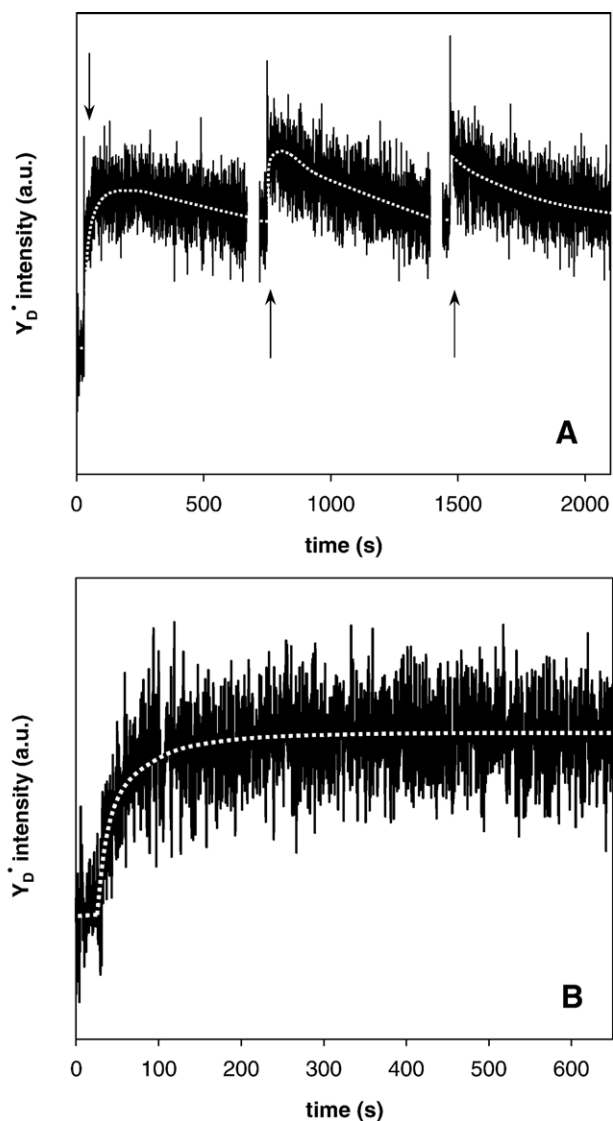


Fig. 2. (A) Formation and decay kinetics of the  $Y_D^{\bullet}$  EPR signal following the application of three consecutive laser flashes at room temperature to PSII-enriched membranes containing PpBQ. The  $Y_D^{\bullet}$  intensity was monitored at the low field peak of  $Y_D^{\bullet}$  (bar in inset in Fig. 1B). The sample had been dark adapted for a total of 20 min before the first flash. Each flash was separated by 12 min in darkness. The application of laser flashes is indicated by arrows. The dashed lines are added for guidance, and do not represent kinetic fits of the data. (B) Subtraction of the kinetic trace after the third flash from the trace after the first flash. This corresponds to the  $Y_D^{\bullet}$  induction component (Eq. (2)) of the first flash trace. (A scaling factor of 0.9 was applied to the third flash prior to the subtraction, to account for the centres that were in the  $Y_D^{\text{red}}S_1$  combination before the first flash.) EPR spectrometer conditions: microwave frequency 9.77 GHz, microwave power 100 mW, modulation amplitude 6 G, modulation frequency 100 kHz, conversion time 328 ms, time constant 82 ms, field position 3462 G (bar in inset, Fig. 1B).

These were thus treated as the synchronising preflashes, and not included in the data sets analysed below.

### 3.3. Kinetic behaviour of the transient increase in $Y_D^{\bullet}$ EPR signal intensity

Fig. 3A shows the flash-induced transient increase of the  $Y_D^{\bullet}$  signal intensity (stage (1)-type) as a function of time, measured

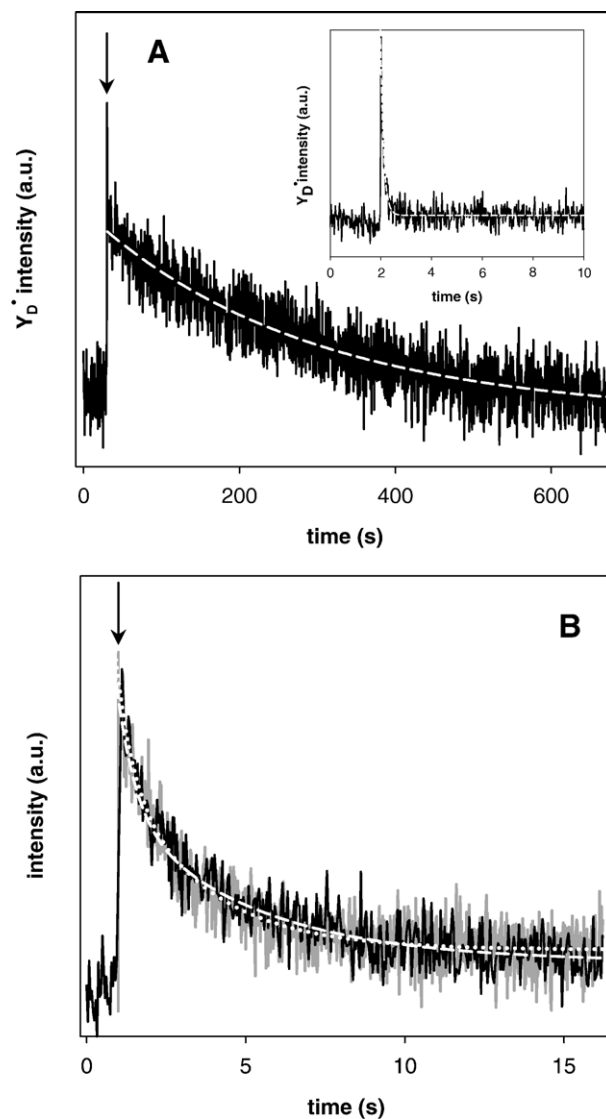


Fig. 3. Kinetic traces of flash-induced changes in the  $Y_D^{\bullet}$  EPR signal intensity recorded at room temperature in PSII-enriched membrane samples containing A: PpBQ and B (dark trace): DCMU. For the trace in the inset of A, a Mn-depleted PSII-enriched membrane in the presence of PpBQ was used. The  $Y_D^{\bullet}$  signal was monitored at the first low field peak position (bar in Fig. 1B inset). A saturating laser flash was applied (arrow) after 30 s for A, and after 1 s for B, with 12 min and 21 s darkness between each flash respectively. For the inset in A, the flash was applied after 2 s. In B, the corresponding flash-induced variable fluorescence decay in PSII-enriched membrane samples containing DCMU (light trace) is overlaid on top of the EPR data. Single exponential fits of the data (dashed line) is shown in A and the inset, and biexponential fits of the EPR (dashed line) and variable fluorescence (dotted line) data are shown in B. EPR spectrometer conditions: microwave power 100 mW, modulation amplitude 6 G, modulation frequency 100 kHz. For A: microwave frequency 9.77 GHz, conversion time 328 ms, time constant 82 ms,  $Y_D^{\bullet}$  monitored at 3462 G, 8 flash transients summed; for the inset in A: microwave frequency 9.77 GHz, conversion time 21 ms, time constant 5 ms,  $Y_D^{\bullet}$  monitored at 3463 G, 40 flash transients summed; for B (dark trace): microwave frequency 9.68 GHz, conversion time 41 ms, time constant 10 ms,  $Y_D^{\bullet}$  monitored at 3431 G, 1200 flash transients summed; for B (light trace): the sum of the first flash transients from 13 independent samples is shown.



at 100 mW microwave power and room temperature, and in the presence of PpBQ as an electron acceptor. At the laser flash (arrow in Fig. 3A), there was an immediate increase in signal intensity, followed by a slow decay to the original level.

The transient increase in amplitude was only observable within the region of the  $Y_D$  spectrum. A corresponding increase in negative amplitude was found when the observed field was poised in the negative regions of the signal, but the flash-induced effect was absent when the observed field was outside of the  $Y_D$  signal (not shown). These observations indicate that the effect was real and directly related to the  $Y_D$  signal. To give some perspective of its overall magnitude, the size of the flash-induced increase was compared with the unsaturated  $Y_D$  signal intensity in the  $S_1$  state. After correcting for the respective EPR measurement parameters, the magnitude of the flash-induced increase was found to be  $\sim 8$ –10% of the original  $Y_D$  low field peak intensity before the flash.

The transient intensity increase began to decay directly after its appearance. Compared to the instantaneous nature of the increase at the laser flash, the decay was very much slower. The  $Y_D$  intensity took close to 10 min to return to the initial baseline intensity. The decay of this flash-induced increase fitted well to a single exponential function, giving a half-life of  $t_{1/2}=200$  s. A biexponential decay fitting was also attempted, giving half-times of 0.49 s and 205 s. However, as the measurement conditions were aimed at obtaining an overall picture of the post-flash decay rather than focussing on very fast processes, we do not draw conclusions regarding the 0.49 s phase, which is close to the conversion time used for data acquisition (328 ms). Confirmation and interpretation of such a fast decay phase is left for further investigations. Therefore, in the present analysis, we consider our results in terms of a single exponential decay.

The same experiment was performed on Mn-depleted PSII-enriched membranes containing PpBQ, again using high applied microwave power (inset in Fig. 3A). While there was also a transient increase at the laser flash, the signal decayed much faster ( $t_{1/2}=87$  ms), which is consistent with  $Y_Z$  formation and re-reduction (see Discussion).

A similar EPR experiment was performed in the presence of DCMU (Fig. 3B, dark trace), which blocks electron transfer from  $Q_A^-$  to  $Q_B$ . This leads to recombination of the  $Q_A^-$  species with the  $CaMn_4$  cluster, now in the  $S_2$  state, after a flash-induced charge separation [30,33,34]. The  $CaMn_4$  cluster is thereby re-reduced to the  $S_1$  state, and no advancement in the S-cycle beyond the  $S_2$  state is possible.

As in the experiments involving PpBQ, it was found that the  $Y_D$  signal increased abruptly when a saturating laser flash was applied to a sample containing DCMU. The observed increase was again instantaneous within our time resolution. A comparison of the flash-induced increase with the  $Y_D$  field scan intensity was performed, as before. In this case, the flash-induced increase was found to be  $\sim 7$ –9% the size of the  $Y_D$  intensity in the  $S_1$  state.

Analogous to the case with PpBQ present, the flash-induced signal increase began to decay immediately after the applied laser flash. But in contrast to samples containing PpBQ, the signal decay back to the baseline level was complete within 10

s. Furthermore, the decay was more obviously biexponential in character, even by visual inspection (Fig. 3B, dark trace). The half-lives of the two decay components were found to be 0.40 s and 2.9 s. The slower decaying phase was somewhat more dominant, contributing to 56% of the overall decay. Due to the more rapid decay of the transient signal increase in the presence of DCMU, the instrumental parameters which were used to observe the overall decay process in this case also allowed the observation of the fast phase with reasonable time resolution (conversion time=41 ms).

### 3.4. $S_2$ multiline signal decay in PpBQ-containing samples

To compare the decay of the flash-induced  $Y_D$  intensity increase (Fig. 3A) with the  $S_2 \rightarrow S_1$  back-reaction process, the decay of the  $S_2$  multiline signal was measured as a function of time after a single-flash. PSII-enriched membrane samples were synchronised using the same preflash protocol as before, and then turned over to the  $S_2$  state by a single laser flash applied at room temperature in the presence of PpBQ. The samples were frozen at different times after the laser flash, and the  $S_2$  multiline signal was measured. Although saturating laser flashes were used (i.e. no more turnover is observed even with increased applied laser power), it is well known that flash turnover inherently involve misses, commonly at 10–15% ([35–37] and references therein) which leads to the damping of the period-of-four cycle in flash-induced oxygen evolution. Therefore illumination at 200 K was subsequently performed on each sample to turn all remaining  $S_1$  state centres to the  $S_2$  state, and the  $S_2$  multiline signal was re-measured to allow normalisation of the data.

Fig. 4A shows that the multiline signal intensity decreased with incubation time after the flash. The decay of the  $S_2$  multiline had a half-life of 215 s (Fig. 4B). This is in good agreement with the  $S_2 \rightarrow S_1$  decay time of 3–3.5 min reported for a similar experiment in the literature [38]. Moreover, for all samples, including the unflash control sample, the post-200 K illumination  $S_2$  multiline signal intensities were identical within experimental errors, indicating that only  $S_1$  and  $S_2$  centres were present in the samples at the time of freezing. Since only the  $S_1 \rightarrow S_2$  transition takes place during illumination at 200 K [38,39], the observed  $S_2$  multiline signal decay can be attributed directly to  $S_2$  centres decaying back to the  $S_1$  state.

The multiline signal decay matches very well with the decay of the flash-induced EPR signal increase in the presence of PpBQ shown in Fig. 3A ( $t_{1/2}=200$  s). Therefore, the flash-induced transient increase in  $Y_D$  intensity and its subsequent decay were directly linked to the formation and re-reduction of the  $S_2$  state.

### 3.5. Variable fluorescence of DCMU-containing samples

Flash-induced variable fluorescence measurements were performed at room temperature (Fig. 3B, light trace) to independently correlate the flash-induced  $Y_D$  signal data obtained in the presence of DCMU. The application of a single flash to an  $S_1$  synchronised sample of PSII-enriched membranes containing DCMU induces

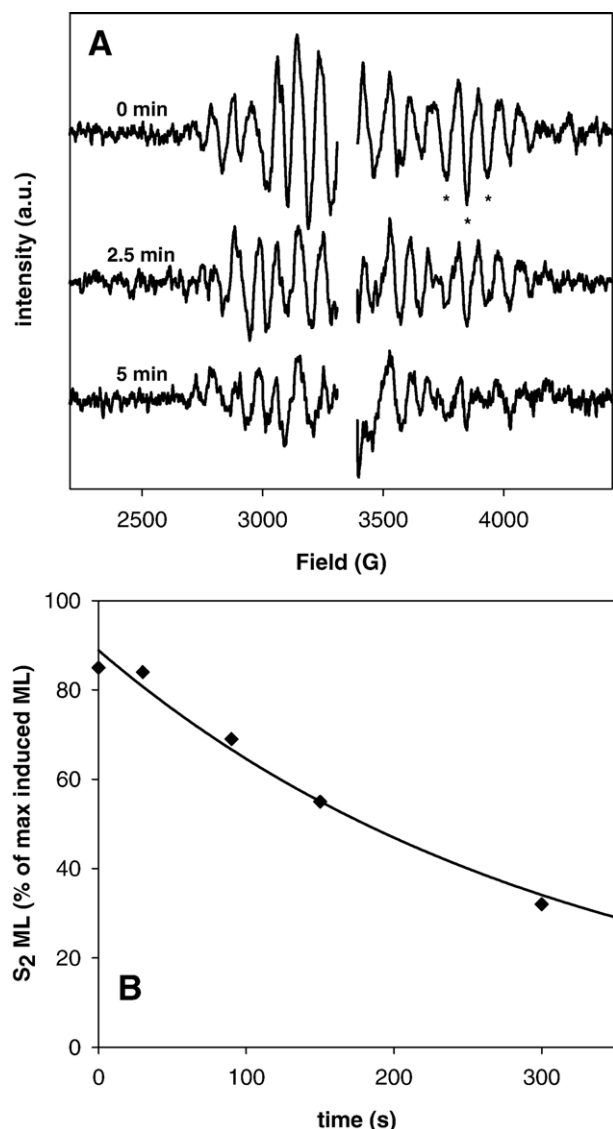


Fig. 4. (A) The decay of the  $S_2$  multiline signal in PSII-enriched membranes containing PpBQ. After the two-flash preflash treatment, the samples were exposed to a single laser flash before being placed in a 23 °C water bath for incubation for various times before freezing. EPR spectrometer conditions: microwave frequency 9.43 GHz, microwave power 16 mW, modulation amplitude 20 G, modulation frequency 100 kHz, temperature 7 K. (B) The  $S_2$  multiline signal amplitude plotted as a function of incubation time. The signal amplitude was measured as the summed amplitudes of the three peaks indicated by asterisks in A. All amplitudes are plotted relative to the 100%  $S_2$  multiline signal which was measured after illumination of each sample at 200 K as described in Materials and methods. All samples were found to give the same maximal, 100%  $S_2$  multiline signal intensity. The data points were fitted to an exponential decay function (solid line).

the  $S_2/Q_A^-$  state, which is highly fluorescent [40]. The decay of this variable fluorescence can therefore be used to follow the recombination reaction back to the  $S_1/Q_A$  state [30,33,34]. The process  $S_1 \xrightarrow{\text{flash}} S_2 \xrightarrow{\text{dark decay}} S_1$  is thus observed.

Upon the application of a single flash, there was an immediate increase in variable fluorescence, indicative of the formation of the  $S_2/Q_A^-$  species. The decay of this signal was very similar to the decay of the corresponding flash-induced  $Y_D^+$  EPR signal. This can be clearly seen in the overlay of the EPR

(dark trace) and variable fluorescence data (light trace) in Fig. 3B. The decay of the variable fluorescence was fitted to a biexponential function, as was done for the EPR data. Half-lives of 0.34 s and 1.8 s were obtained, which are similar to those obtained for the EPR experiment. These values are also consistent with literature reports of  $S_2/Q_A^-$  recombination in the presence of DCMU and can be safely assigned to this process [30,34,41]. Furthermore, it was found that the slower decaying phase was dominant, comprising 65% of the overall signal decay. This is again similar to the EPR data obtained from in DCMU-containing samples.

These results demonstrate once again that the  $S_2$  state is responsible for producing the flash-induced effect on the  $Y_D^+$  EPR signal, this time in the presence of DCMU. This is in agreement with the experiments above conducted in the presence of PpBQ.

## 4. Discussion

### 4.1. Flash-induced transient increase in $Y_D^+$ intensity

Looking at the results from samples containing PpBQ (Fig. 3A), several processes could be immediately excluded from causing the observed flash-induced transient increase in  $Y_D^+$  intensity. Firstly, formation and re-reduction of  $Y_D^+$  could be excluded from being the cause. Although both  $Y_D^+$  and  $Y_Z^+$  are tyrosine radicals, so that their steady state EPR signals are almost identical and can be easily confused,  $Y_Z^+$  is re-reduced to  $Y_Z$  by the OEC in the microsecond to millisecond time scale where the OEC is intact [42–44]. This is much faster than the decay reactions studied here. This also holds true for Mn-depleted PSII, where  $Y_Z^+$  decays with  $t_{1/2} \approx 50\text{--}1000$  ms [45–47]. This decay rate was shown to be unaffected by the use of high applied microwave power in the control experiment shown in the inset of Fig. 3A. A half-life of  $t_{1/2} = 87$  ms was obtained. This experiment also demonstrated that the  $\text{CaMn}_4$  cluster was required for the  $t_{1/2} = 200$  s decay to be observed. Therefore, regardless of whether the OEC was intact or not, the observed decay in Fig. 3A was too long to be due to  $Y_Z^+$  decay.

The half-time of 200 s was also too rapid for it to represent ordinary reduction of  $Y_D^+$  to  $Y_D$ . This decay is known to take place over many hours in intact PSII in the  $S_1$  state [28,31,48] (also confirmed in our study; not shown). Moreover, the flash-induced intensity increase always returned to the baseline, pre-flash level in the dark. This baseline level represents the starting  $Y_D^+$  intensity, and it remained stable over many hours (full initial oxidation of  $Y_D$  to  $Y_D^+$  and its maintenance was achieved and verified; see below). Therefore, the  $t_{1/2} = 200$  s, flash-induced transient intensity increase represents some other effect that was superimposed onto the otherwise stable  $Y_D^+$  radical signal.

### 4.2. Involvement of the $S_2$ state

From the above, we can conclude that the effect did not involve a change in the oxidation state of the  $Y_Z$  or  $Y_D$  residues. Instead, several factors indicated that it was instead related to a flash-induced  $S_1 \rightarrow S_2$  turnover and the subsequent  $S_2 \rightarrow S_1$  back-

reaction. Firstly, the effect could be repeatedly triggered with single laser flashes when interspersed with an appropriate dark adaptation period. Secondly, the increase in  $Y_D$  intensity is instantaneous on the timescale of the kinetic measurements and occurs simultaneously with the laser flash. This is consistent with the change being associated with the very rapid formation of the  $S_2$  state. Thirdly, the lifetime of this decay was much longer in the presence of PpBQ, which is known to stabilise the higher S-states of the OEC [38], than in the presence of DCMU, which by contrast promotes fast recombination after charge separation [30,33,34]. Fourthly, in samples containing DCMU, the OEC is restricted to the  $S_1$  and  $S_2$  states. Finally, the flash-induced transient increase was only observed at high microwave powers and did not become saturated even where the  $Y_D$  signal was otherwise saturated (Fig. 1B). Considering these various factors, we propose that the intensity increase is consistent with the flash-induced  $S_2$  state being a faster (spin) relaxer of the  $Y_D$  radical than the  $S_1$  state, leading to the increased  $Y_D$  EPR intensity.

This hypothesis was confirmed with the control experiments involving  $S_2$  multiline decay in the presence of PpBQ, and flash-induced variable fluorescence in the presence of DCMU (Figs. 4B and 3B, respectively). The former can be likened to taking frozen snap-shots of the  $S_1$  vs.  $S_2$  state distribution as a function of decay time at room temperature, while the latter is indicative of the  $S_2/Q_A^-$  recombination. The fact that in both cases the lifetimes obtained from these independent experiments correlated so well with their respective EPR experiments is remarkable, given that the mechanisms for  $S_2 \rightarrow S_1$  decay in the presence of PpBQ and DCMU are quite different from each other. They provide clear evidence that the mutual link of the experiments, the formation and decay of the  $S_2$  state, is responsible of the flash-induced EPR intensity increase and subsequent decay of the  $Y_D$  signal.

#### 4.3. Enhanced spin relaxation of $Y_D$ by the $S_2$ state

These experiments confirmed that the S-state dependence of  $Y_D$  spin relaxation rate, which previously has only been studied at low temperatures (4–25 K), could be used as a passive probe for the kinetic observation of reactions in S-cycle at room temperature. De Groot et al. [16] first deduced, from spin-echo studies performed at 5 K, that the spin-relaxation time of  $Y_D$  varied with the S-state and intactness of the OEC. The authors proposed that spin-lattice relaxation of  $Y_D$  was most likely influenced by the Mn cluster in the OEC.

Styring and Rutherford extended this [17] in a microwave power saturation study using laser-flashed PSII samples poised at different S-states with a well-defined composition. The  $Y_D$  signal relaxed differently in each of the four S-states, and the results were temperature dependent. At 8 K, the trend in  $P_{1/2}$  values for PSII-enriched membranes was  $S_1 < S_2 = S_3 < S_0$ , whereas the pattern was  $S_1 < S_0 < S_3 \approx S_2$  at 20 K. Similar results were obtained in spin-echo EPR studies by Evelo et al. [18], who also demonstrated the complex dependence of the spin-lattice relaxation rate on flash number and temperature. In each case, the  $S_2$  state was shown to be a faster relaxer of the  $Y_D$  radical than the  $S_1$  state. After the discovery of the multiline

signal in the  $S_0$  state, Peterson et al. [19] were also able to directly correlate these trends with the power saturation of the  $CaMn_4$  cluster of the OEC in  $S_0$  and  $S_2$  states.

While it has been shown that high-spin non-heme  $Fe^{2+}$  in PSII also contributes to the changes in  $Y_D$  relaxation behaviour [21–23,49], the influence of the Mn cluster has been shown to be much greater [23,24]. In addition, the distance between the  $Y_D$  and the OEC is  $\sim 30$  Å [5–8], which is a reasonable distance for magnetic interaction between two species.

In the present study, an indicator that the flash-induced effects of the  $Y_D$  signal were due to the  $S_2$  state causing faster  $Y_D$  spin relaxation was that the effect could only be observed under saturating microwave power. As discussed above, the rate of spin relaxation becomes determinative of the maximum signal intensity of a radical at saturating microwave powers. If the effect had simply reflected an increase in the number of  $Y_D$  spins, with unaltered relaxation behaviour, an increase in signal would be expected at all microwave powers, with the magnitude of increase directly proportional to the increase in observable electron spins.

This power-dependent behaviour was observed at room temperature in this study (Fig. 1). In particular, the fact that the magnitude of the flash-induced effect continued to increase even at microwave powers where the  $Y_D$  signal was saturated ( $> \sim 30$  mW) was further evidence that the effect was not due to extra spins being induced in the sample, but rather dependent on an increase in the  $Y_D$  relaxation rate. Significantly, Styring and Rutherford [38] have also reported a decrease in the microwave power at half-saturation of  $Y_D$  at 20 K which correlated with the decay of the  $S_2$  multiline signal of the sample.

In summary, the  $Y_D$  intensity kinetic traces measured at room temperature as shown in Fig. 3 can be interpreted as follows. Before the application of the laser flash, the baseline level represents  $Y_D$  intensity under the  $S_1$  state of the OEC. At the laser flash, turnover to the  $S_2$  state is induced. As the  $S_2$  state is a faster spin relaxer of  $Y_D$  than the  $S_1$  state, this causes an immediate jump in  $Y_D$  intensity when recorded at the high microwave power used. As the  $S_2$  state centres decay back to the  $S_1$  state, the  $Y_D$  intensity decreases again to baseline levels.

#### 4.4. Role and efficiency of preflashes

While the traditional single preflash/dark adaptation protocol does give full  $S_1$  state synchronisation [9,28,29] (c.f. [50], where a two-flash preflash protocol was briefly described), the fate of  $Y_D$  also needed to be considered in the current study in order to avoid experimental artefacts from trivial  $Y_D$  formation. Most notably, apart from the centres in the  $S_2$  and  $S_3$  states decaying back to the dark-stable  $S_1$  state, the following reaction is known to take place during initial dark adaptation following exposure of PSII-membranes to room light [28] (superscript “red” for reduced  $Y_D$  added here for clarity):



Thus, there are three  $Y_D$ /S-state combinations before the application of the preflash, namely  $Y_D^{\bullet} S_0$ ,  $Y_D^{\bullet} S_1$  and  $Y_D^{\text{red}} S_1$ . A



single saturating preflash then generates  $Y_D^+S_1$ ,  $Y_D^+S_2$  and  $Y_D^{red}S_2$ . Of these,  $Y_D^+S_1$  is stable, and  $Y_D^+S_2$  decays back to  $Y_D^+S_1$ . Two pathways are available for  $Y_D^{red}S_2$  decay:



Eq. (2) shows the active reduction of the  $S_2$  state by  $Y_D^{red}$ , so that some of reduced  $Y_D$  is recovered [31,32,49,51], whereas Eq. (3) represents passive decay of  $S_2$  to  $S_1$  without the participation of  $Y_D^{red}$ . Although the “active” process is faster than the “passive” ( $t_{1/2}=10\text{--}12\text{ s}$  [31,32] and  $t_{1/2}=3\text{--}3.5\text{ min}$  [38], respectively), these are competing processes, and a certain fraction of the sample would remain in the  $Y_D^{red}S_1$  combination. As more preflashes are applied, these centres represent an ever diminishing proportion of the sample.<sup>1</sup>

The observed behaviour of the  $Y_D$  amplitude after the first three flashes (Fig. 2A) is in excellent correspondence to this analysis. After the first flash, there is a significant and persistent increase in  $Y_D$  intensity which does not return to the baseline value, indicating the formation of extra  $Y_D$  in accordance to Eq. (2). This was also visible to a smaller extent after the second flash, as expected from the above analysis, and manifested itself only as a slight curvature in the post-flash decay. By the third flash, only the transient flash-induced  $Y_D$  intensity increase was present (c.f. Fig. 3A), indicating that full oxidation to  $Y_D^+$  had been achieved. Subtracting the trace after the third flash from that after the first flash (Fig. 2B), an increase in  $Y_D$  intensity with a half-time of  $t_{1/2} \sim 25\text{ s}$  was found. Both the shape and  $t_{1/2}$  of this growth kinetic are similar to literature reports of the induction of  $Y_D$  involving the  $S_2$  state as represented in Eq. (2) [31,32]. Therefore, we could be confident that all  $Y_D$  was oxidised using the two-flash preflash protocol, and the observed flash-induced changes in  $Y_D$  intensity (Fig. 3) were not associated with trivial re-oxidation of residual  $Y_D$  in the sample.

## 5. Conclusions

In this study, we have demonstrated that the EPR signal of  $Y_D$  undergoes a transient increase in intensity upon the application of a laser flash to an  $S_1$ -state synchronised PSII-enriched membrane sample. This increase occurs concomitantly with the flash-induced turnover of  $\text{CaMn}_4$  cluster to the  $S_2$  state, and can be repeatedly triggered. The decay kinetics of  $Y_D$  signal intensity back to baseline levels was compared with independent experiments involving  $S_2$  multiline signal decay in the presence of PpBQ, as well as flash-induced variable fluorescence decay in the presence of DCMU. The close correspon-

dence between the EPR and non-EPR experiments indicated that the post-flash  $Y_D$  signal decay reflected  $S_2 \rightarrow S_1$  back-turnover of the  $\text{CaMn}_4$  cluster. By excluding other processes involving changes in  $Y_Z$  and  $Y_D$  oxidation states as sources of the observed transient increase, and taking into account literature studies of S-state dependent  $Y_D$  spin relaxation enhancement, we conclude that this effect can be attributed to the  $S_2$  state acting as a faster relaxer of  $Y_D$  than the  $S_1$  state. Thus, we have demonstrated the ability to observe and follow this effect kinetically at room temperature, in contrast to previous studies at cryogenic temperatures.

At present, there are few methods available for kinetic studies of S-state turnovers and the associated magnetic changes within the OEC which either directly observe the  $\text{CaMn}_4$  cluster, or is independent of a subsequent reaction, such as  $Y_Z^-$  reduction (e.g. [9,52,53]). Further investigations of this  $Y_D$  relaxation enhancement effect provides such an opportunity, as  $Y_D$  acts as a passive probe to sense the changes within the OEC without the involvement of some other reaction. Given that previous studies have also shown higher  $Y_D$  spin relaxation rates in the presence of the  $S_3$  and  $S_0$  states, the application of multiple laser flashes would allow the study of these S-states of the OEC as well. In addition, the ability to study the S-state turnover and back-reactions kinetically is particularly desirable. For example, with sufficiently high time resolution, it may be possible to detect intermediates during individual S-state transitions. Also, by varying other parameters such as temperature and pH, it would be possible to directly follow how the transitions and back-reactions are affected or even inhibited by these factors. In this way, new insight could be gained about the details of the mechanisms of water oxidation.

## Acknowledgements

The financial support from the Swedish Research Council, the Knut and Alice Wallenberg Foundation, the Swedish Energy Agency, and the European Community Sixth Framework Programme, Marie Curie Incoming International Fellowship (514817 to FMH) is gratefully acknowledged.

## References

- [1] J. Nugent (Ed.), Photosynthetic Water Oxidation, Biochim. Biophys. Acta, vol. 1503, 2001, Special issue.
- [2] J. Messinger, W. Lubitz (Eds.), Biophysical Studies on Photosystem II and Related Model Systems, Phys. Chem. Chem. Phys., vol. 6, 2004, Special issue.
- [3] G. Renger, Photosynthetic water oxidation to molecular oxygen: apparatus and mechanism, Biochim. Biophys. Acta 1503 (2001) 210–228.
- [4] C. Goussias, A. Boussac, A.W. Rutherford, Photosystem II and photosynthetic oxidation of water: an overview, Philos. Trans. R. Soc. Lond., B 357 (2002) 1369–1381.
- [5] A. Zouni, H.T. Witt, J. Kern, P. Fromme, N. Krauss, W. Saenger, P. Orth, Crystal structure of photosystem II from *Synechococcus elongatus* at 3.8 Å resolution, Nature 409 (2001) 739–743.
- [6] N. Kamiya, J.R. Shen, Crystal structure of oxygen-evolving photosystem II from *Thermosynechococcus vulcanus* at 3.7 Å resolution, Proc. Natl. Acad. Sci. U. S. A. 100 (2003) 98–103.

<sup>1</sup> Misses inherent in the flash turnover has not been included in the discussion. The only species not accounted for after the first flash and its subsequent dark adaptation is a very small amount of stable  $Y_D^+S_0$ , present in only 1–2% of the total number of centres. By the second flash, this would be reduced to 0.1–0.2% of the centres. This does not significantly affect our analysis.



- [7] K.N. Ferreira, T.M. Iverson, K. Maghlaoui, J. Barber, S. Iwata, Architecture of the photosynthetic oxygen-evolving center, *Science* 303 (2004) 1831–1838.
- [8] B. Loll, J. Kern, W. Saenger, A. Zouni, J. Biesiadka, Towards complete cofactor arrangement in the 3.0 Å resolution structure of photosystem II, *Nature* 438 (2005) 1040–1044.
- [9] M. Haumann, C. Müller, P. Liebisch, L. Iuzzolino, J. Dittmer, M. Grabolle, T. Neisius, W. Meyer-Klaucke, H. Dau, Structural and oxidation state changes of the photosystem II manganese complex in four transitions of the water oxidation cycle ( $S_0 \rightarrow S_1$ ,  $S_1 \rightarrow S_2$ ,  $S_2 \rightarrow S_3$ , and  $S_3 \rightarrow S_0$ ) Characterized by X-ray absorption spectroscopy at 20 K and room temperature, *Biochemistry* 44 (2005) 1894–1908.
- [10] M. Haumann, P. Liebisch, C. Müller, M. Barra, M. Grabolle, H. Dau, Photosynthetic  $O_2$  formation tracked by time-resolved X-ray experiments, *Science* 310 (2005) 1019–1021.
- [11] J. Clausen, W. Junge, Detection of an intermediate of photosynthetic water oxidation, *Nature* 430 (2005) 480–483.
- [12] W. Junge, J. Clausen, J.E. Penner-Hahn, C.F. Yocum, H. Dau, M. Haumann, Photosynthetic oxygen production, *Science* 312 (2006) 1470–1472.
- [13] C.W. Hoganson, G.T. Babcock, Photosystem, in: M. Sigel, A. Sigel (Eds.), *Metalloenzymes Involving Amino Acid—Residue and Related Radicals, Metal Ions in Biological System*, vol. 30, Marcel Dekker Ltd, New York, 1994, pp. 77–107.
- [14] A.W. Rutherford, A. Boussac, P. Faller, The stable tyrosyl radical in Photosystem II: why D? *Biochim. Biophys. Acta* 1655 (2004) 222–230.
- [15] B.A. Diner, R.D. Britt, The redox-active tyrosines  $Y_Z$  and  $Y_D$ , in: T.J. Wydrzynski, K. Satoh (Eds.), *Photosystem II: The Light-Driven Water: Plastoquinone Oxidoreductase*, Springer, Dordrecht, The Netherlands, 2005, pp. 207–233.
- [16] A. de Groot, J.J. Plijter, R. Evelo, G.T. Babcock, A.J. Hoff, The influence of the oxidation state of the oxygen-evolving complex of Photosystem II on the spin-lattice relaxation time of Signal II as determined by electron spin-echo spectroscopy, *Biochim. Biophys. Acta* 848 (1986) 8–15.
- [17] S.A. Styring, A.W. Rutherford, The microwave power saturation of  $S_{II,slow}$  varies with the redox state of the oxygen-evolving complex in Photosystem II, *Biochemistry* 27 (1988) 4915–4923.
- [18] R.G. Evelo, S. Styring, A.W. Rutherford, A.J. Hoff, EPR relaxation measurements of Photosystem II reaction centers: influence of S-state oxidation and temperature, *Biochim. Biophys. Acta* 973 (1989) 428–442.
- [19] S. Peterson, K.A. Åhring, S. Styring, The EPR signals from the  $S_0$  and  $S_2$  states of the Mn cluster in Photosystem II relax differently, *Biochemistry* 38 (1999) 15223–15230.
- [20] S. Peterson, K.A. Åhring, J.E.P. Höglblom, S. Styring, Flash-induced relaxation changes of the EPR signals from the manganese cluster and  $Y_D$  reveal a light-adaptation process of Photosystem II, *Biochemistry* 42 (2003) 2748–2758.
- [21] W.F. Beck, J.B. Innes, G.W. Brudvig, Electron spin-lattice relaxation of the stable tyrosine radical  $D^{\bullet}$  in Photosystem, in: M. Baltscheffsky (Ed.), *Current Research in Photosynthesis*, vol. 1, Kluwer Academic Publishers, Dordrecht, The Netherlands, 1990, pp. 817–820.
- [22] D.J. Hirsh, W.F. Beck, J. Innes, G.W. Brudvig, Using saturation-recovery EPR to measure distances in proteins: applications to Photosystem II, *Biochemistry* 31 (1992) 532–541.
- [23] D. Kouloulgiotis, R.H. Schweitzer, G.W. Brudvig, The tetranuclear manganese cluster in Photosystem II: location and magnetic properties of the  $S_2$  state as determined by saturation-recovery EPR spectroscopy, *Biochemistry* 36 (1997) 9735–9746.
- [24] M.K. Bosch, R.G. Evelo, S. Styring, A.W. Rutherford, A.J. Hoff, ESE relaxation measurements in photosystem II. The influence of the reaction center non-heme iron on the spin-lattice relaxation of Tyr  $D^{\bullet}$ , *FEBS Lett.* 292 (1991) 279–283.
- [25] D.A. Berthold, G.T. Babcock, C.F. Yocum, A highly resolved, oxygen-evolving Photosystem II preparation from spinach thylakoid membranes: EPR and electron-transport properties, *FEBS Lett.* 134 (1981) 231–234.
- [26] R.J. Pace, P. Smith, R. Bramley, D. Stehlik, EPR saturation and temperature-dependence studies on signals from the oxygen-evolving center of Photosystem-II, *Biochim. Biophys. Acta* 1058 (1991) 161–170.
- [27] R.E. Blankenship, K. Sauer, Manganese in photosynthetic oxygen evolution. I: electron paramagnetic resonance study of the environment of manganese in Tris-washed chloroplasts, *Biochim. Biophys. Acta* 357 (1974) 252–266.
- [28] S. Styring, A.W. Rutherford, In the oxygen-evolving complex of Photosystem II the  $S_0$  state is oxidized to the  $S_1$  state by  $D^+$  (Signal  $II_{slow}$ ), *Biochemistry* 26 (1987) 2401–2405.
- [29] K.A. Åhring, S. Peterson, S. Styring, An oscillating manganese electron paramagnetic resonance signal from the  $S_0$  state of the oxygen evolving complex in Photosystem II, *Biochemistry* 36 (1997) 13148–13152.
- [30] F. Mamedov, H. Stefansson, P.-Å. Albertsson, S. Styring, Photosystem II in different parts of the thylakoid membrane: a functional comparison between different domains, *Biochemistry* 39 (2000) 10478–10486.
- [31] I. Vass, S. Styring, pH-Dependent charge equilibria between tyrosine-D and the S states in Photosystem II. Estimation of relative midpoint redox potentials, *Biochemistry* 30 (1991) 830–839.
- [32] Z. Deák, I. Vass, S. Styring, Redox interaction of tyrosine-D with the S-states of the water-oxidizing complex in intact and chloride-depleted photosystem, *Biochim. Biophys. Acta* 1185 (1994) 65–74.
- [33] P. Joliot, A. Joliot, B. Bouges, B. Barbieri, Studies of system-II photocenters by comparative measurements of luminescence, fluorescence and oxygen emission, *Photochem. Photobiol.* 14 (1971) 287–305.
- [34] K.G.V. Sigfridsson, G. Bernát, F. Mamedov, S. Styring, Molecular interference of  $Cd^{2+}$  with Photosystem II, *Biochim. Biophys. Acta* 1659 (2004) 19–31.
- [35] G. Bernát, F. Morvaridi, Y. Feyziyev, S. Styring, pH Dependence of the four individual transitions in the catalytic S-cycle during photosynthetic oxygen evolution, *Biochemistry* 41 (2002) 5830–5843.
- [36] V.P. Shinkarev, Flash-induced oxygen evolution in photosynthesis: simple solution for the extended S state model that includes misses, double-hits, inactivation, and backward transitions, *Biophys. J.* 88 (2005) 412–421.
- [37] R. de Wijn, H.J. van Gorkom, S state dependence of the miss probability in Photosystem II, *Photosynth. Res.* 72 (2002) 217–222.
- [38] S. Styring, A.W. Rutherford, Deactivation kinetics and temperature dependence of the S-state transitions in the oxygen-evolving system of Photosystem II measured by EPR spectroscopy, *Biochim. Biophys. Acta* 933 (1988) 378–387.
- [39] G.W. Brudvig, J.L. Casey, K. Sauer, The effect of temperature on the formation and decay of the multiline EPR signal species associated with photosynthetic oxygen evolution, *Biochim. Biophys. Acta* 723 (1983) 366–371.
- [40] G.H. Krause, E. Weis, Chlorophyll fluorescence and photosynthesis: the basics, *Annu. Rev. Plant Physiol. Plant Mol. Biol.* 42 (1991) 313–349.
- [41] F. Mamedov, E. Rintamäki, E.-M. Aro, B. Andersson, S. Styring, Influence of protein phosphorylation on the electron-transport properties of Photosystem II, *Photosynth. Res.* 74 (2000) 61–72.
- [42] G.T. Babcock, R.E. Blankenship, K. Sauer, Reaction kinetics for positive charge accumulation on the water side of chloroplast Photosystem II, *FEBS Lett.* 61 (1976) 286–289.
- [43] S. Gerken, K. Brettel, E. Schlodder, H.T. Witt, Optical characterization of the immediate electron donor to chlorophyll  $a_{II}^+$  in  $O_2$ -evolving photosystem II complexes. Tyrosine as possible electron carrier between chlorophyll  $a_{II}$  and the water-oxidizing manganese complex, *FEBS Lett.* 237 (1988) 69–75.
- [44] M.R. Razeghifard, R.J. Pace, Electron paramagnetic resonance kinetic studies of the S states in spinach PSII membranes, *Biochim. Biophys. Acta* 1322 (1997) 141–150.
- [45] J.T. Warden, R.E. Blankenship, K. Sauer, A flash photolysis ESR study of Photosystem II signal  $II_{vF}$ , the physiological donor to  $P-680^+$ , *Biochim. Biophys. Acta* 423 (1976) 462–478.
- [46] R.A. Roffey, K.J. van Wijk, R.T. Sayre, S. Styring, Spectroscopic characterization of Tyrosine-Z in Histidine 190 mutants of the D1 protein in Photosystem II (PSII) in *Chlamydomonas reinhardtii*, *J. Biol. Chem.* 269 (1994) 5115–5121.
- [47] P. Faller, R.J. Debus, K. Brettel, M. Sugiura, A.W. Rutherford, A. Boussac, Rapid formation of the stable tyrosyl radical in photosystem II, *Proc. Natl. Acad. Sci. U. S. A.* 98 (2001) 14368–14373.
- [48] G.T. Babcock, K. Sauer, Electron paramagnetic resonance Signal II in

- spinach chloroplasts. I. Kinetic analysis for untreated chloroplasts, *Biochim. Biophys. Acta* 325 (1973) 483–503.
- [49] D. Koulougliotis, X.-S. Tang, B.A. Diner, G.W. Brudvig, Spectroscopic evidence for the symmetric location of tyrosines D and Z in Photosystem II, *Biochemistry* 34 (1995) 2850–2856.
- [50] T.A. Roelofs, W. Liang, M.J. Latimer, R.M. Cinco, A. Rompel, J.C. Andrews, K. Sauer, V. Yachandra, M.P. Klein, Oxidation states of the manganese cluster during the flash-induced S-state cycle of the photosynthetic oxygen-evolving complex, *Proc. Natl. Acad. Sci. U. S. A.* 93 (1996) 3335–3340.
- [51] Y. Feyziyev, B.J. van Rotterdam, G. Bernát, S. Styring, Electron transfer from cytochrome  $b_{559}$  and tyrosine<sub>D</sub> to the  $S_2$  and  $S_3$  states of the water oxidizing complex in photosystem II, *Chem. Phys.* 294 (2003) 415–431.
- [52] Ö. Saygin, H.T. Witt, Optical characterization of intermediates in the water-splitting enzyme system of photosynthesis—Possible states and configurations of manganese and water, *Biochim. Biophys. Acta* 893 (1987) 452–469.
- [53] P.J. van Leeuwen, C. Heimann, H.J. van Gorkom, Absorbance difference spectra of the S-state transitions in Photosystem II core particles, *Photosynth. Res.* 38 (1993) 323–330.